A kinetic study of the plasma-etching process. I. A model for the etching of Si and SiO_2 in C_nF_m/H_2 and C_nF_m/O_2 plasmas

M. J. Kushner[a)]
Sandia National Laboratories, Division 4216, Albuquerque, New Mexico 87185

(Received 23 July 1981; accepted for publication 15 December 1981)

A kinetic model of the plasma-etching process has been developed to describe the etching of Si and SiO_2 in C_nF_m/O_2 and C_nF_m/H_2 plasmas ($C_nF_m \equiv CF_4$, C_2F_6). The model has obtained good agreement with experiment for demonstrating the selective etching of SiO_2 in C_nF_m/H_2 plasmas, and the enhancement of the etch rate of Si in C_nF_m/O_2 plasmas. Good agreement is also obtained with mass spectroscopic measurements of neutral species from a CF_4/H_2 plasma. Results from the model indicate that the adsorption of atomic hydrogen on silicon surfaces from C_nF_m/H_2 plasmas, which then reacts with adsorbed fluorine, can significantly affect the selectivity of etching SiO_2 with respect to Si. Similarly, the adsorption of atomic oxygen, which then reacts with adsorbed carbon thereby cleansing the surface, may be responsible for the large etch rates of Si seen in C_nF_m/O_2 plasmas. The selectivity of etching SiO_2 in C_nF_m/H_2 plasmas has been found to be a sensitive function of the C/F ratio of the carbon-bearing molecules which desorb from the surface, and a C/F ratio of 0.5 shows best agreement with experiment. Results from the model favor ion drift as a dominant mechanism by which radicals are transported to the surface.

PACS numbers: 52.40.Hf, 52.80.Pi, 82.65.Nz, 82.20.Wt

I. INTRODUCTION

Plasma etching is a process by which micron- and submicron-dimensioned features can be fabricated for semiconductor devices.[1–6] In a low pressure ($\leqslant 100$ mTorr), radio frequency discharge, fluorine-containing gases, are dissociated to form both neutral and ionic radicals. These radicals diffuse or are accelerated toward the semiconductor surface where they are adsorbed. Atoms from the radicals bond with the lattice atoms and are desorbed as a volatile gas which is then pumped away. For example, silicon is rapidly etched by carbon tetrafluoride plasmas (CF_4) producing the volatile product silicon tetrafluoride (SiF_4). There are many advantages to plasma etching over the traditional liquid etches. Some of these are high resolution, anisotropic (straight wall) features, and the elimination of large volumes of caustic liquids. The largest drawback to the process is its lack of selectivity; that is, the ability for the etching process to distinguish between silicon and its compounds. This is especially important when one desires to etch a contact window through a silicon oxide layer to the silicon layer below.

It has been determined that the ratio of reactive carbon to fluorine in the plasma (i.e., the C/F ratio) is important in determining the selectivity of the etching process.[7] When etching silicon, carbon is adsorbed on the surface when radicals such as CF_3 are adsorbed. This carbon must be desorbed by forming a compound such as CF_4. The fluorine atoms which are used to make the CF_4 reduce the number of adsorbed fluorine atoms which might otherwise etch the silicon by bonding with a silicon atom and be desorbed as SiF_4. Failure to remove the adsorbed carbon leads to a polymer forming on the surface which results in the termination of the etching process. Therefore low C/F ratios favor etching silicon. The opposite is true for etching silicon dioxide (SiO_2). In the case of the oxide, carbon is necessarily adsorbed on the surface in order to bond with the lattice oxygen and be desorbed as an oxygen-bearing molecule (e.g., CO, CO_2, COF_2). Therefore large C/F ratios favor etching SiO_2 with respect to Si.

Although many attempts have been made to quantify the plasma-etching process, it still remains largely an empirical art. This is due primarily to the large parameter space and interdependence of those parameters which make interpreting experimental results difficult. For example, it has been found that the use of additive gases with CF_4 or C_2F_6 can alter the C/F ratio of the reactive species and thereby change the selectivity of the etching process. Specifically, CF_4/H_2 mixtures increase the selectivity of etching SiO_2 with respect to silicon,[8] while CF_4/O_2 mixtures do the opposite.[9] The relative abundance of radical species when additive gases are used has been measured, primarily with mass spectroscopy.[9–13] Optical observations of fluorescence have been made,[9,14–16] and specifics of chemisorption of radical species as pertains to plasma etching have also been investigated.[17] A limited number of electrical probe studies have also been carried out.[18–20]

To quantitatively describe the plasma-etching process, one must consider electron-impact events, ion chemistry, neutral gas-phase reactions, diffusion, space-charge effects, adsorption, desorption, and the actual etching process. In their paper, Winters *et al.*[21] used a "pseudo-black-box" approach to quantitatively describe the process. They included many of the particulars described above in an *ad hoc* fashion and were successful in reproducing many systematic trends.

In this paper, a kinetic model of the plasma-etching process is presented which quantitatively describes the etch-

[a)]Present address: Lawrence Livermore National Laboratory, University of California, MS-L467, Livermore, CA 94550.

 0021/8979/82/042923-16$02.40 © 1982 American Institute of Physics

Downloaded 27 Mar 2003 to 128.174.115.149. Redistribution subject to AIP license or copyright, see http://ojps.aip.org/japo/japcr.jsp

ing of silicon compounds by considering all of the processes listed above. In a companion paper,[22] electrical probe measurements made in a plasma-etching reactor under actual operating conditions will be discussed in view of the results presented here. The model will be described in Sec. II. Results from the model for the etching process in C_nF_m/H_2 plasmas will be discussed in Sec. III and for C_nF_m/O_2 plasmas in Sec. IV. Section V discusses the effect of ions on the etching process, and Sec. VI contains concluding remarks.

II. DESCRIPTION OF THE MODEL

The calculation simulates a radio-frequency (rf) discharge between two large parallel plates by considering electron-impact events, ion chemistry, neutral chemistry, radical transport, adsorption, desorption, and etching. The flux of radicals incident on the surface to be etched is calculated; a fraction are adsorbed on the surface. Depending on the specific surface, products are desorbed and returned to the plasma (see Fig. 1).

Unlike conventional steady-state discharges, rf plasmas can be very hot, with electron temperatures from a few to tens of electron volts.[22,23] This is a result of the large electric field that can be applied to a typical plasma-etching discharge. A laboratory gas laser may have an average E/P (electric field divided by gas pressure) as high as 10 V/cm Torr. A 100 W rf plasma-etching discharge may have an applied E/P of 2500 V/cm Torr although a large fraction of the applied voltage is shielded from the plasma by sheaths at the electrodes or walls. Conventional steady-state discharges usually rely on some electrode phenomenon (e.g., cathode secondary-electron emission) to be sustained. A high-frequency rf discharge (>10 MHz) can be sustained independent of electrode phenomenon. High electron densities and temperatures are possible due to the oscillation of the applied electric field. The oscillation confines the drift of electrons, keeping them away from surfaces where they might recombine. A large space-charge field develops which forms a potential well for the electrons and protects the plasma from the walls. The high electron temperatures and densities add to the complexity of the system by rapidly stripping the input gases of atoms, creating a variety of radicals.

TABLE I. Species in the model.

Input gases	Neutral radicals
CF_4	CF_3 F SiF_3 COF
C_2F_6	CF_2 H SiF_2 OH
H_2	CF O SiF OF
O_2	C
Stable products	**Charged species**
C_2F_4 F_2 CO	CF_3^+ H_2^+ CF_3^- e
C_2F_2 HF CO_2	CF_2^+ H^+ O_2^-
SiF_4 H_2O COF_2	CF^+ O_2^+ O^-
CHF_3	F^+ O^+

The species included in the model are listed in Table I. The choice of species was dominated by the reaction mechanisms proposed by previous investigators and by the most probable electron-impact events which might occur.

The calculation begins with solving for the electron-distribution function based on the properties of the input gases. Quasi-steady-state conditions are assumed with an average electric field. The electron-distribution calculation is a solution of Boltzmann's equation in finite-difference form. The specific form of the solution is based on an adaption of the program described in detail in Ref. 24. The solution is, at best, an approximation due to two main causes. First, a large fraction of the input gases is dissociated, and the products of those dissociations are ignored in calculating the distribution function. Secondly, many of the electron-impact cross sections are approximations themselves.

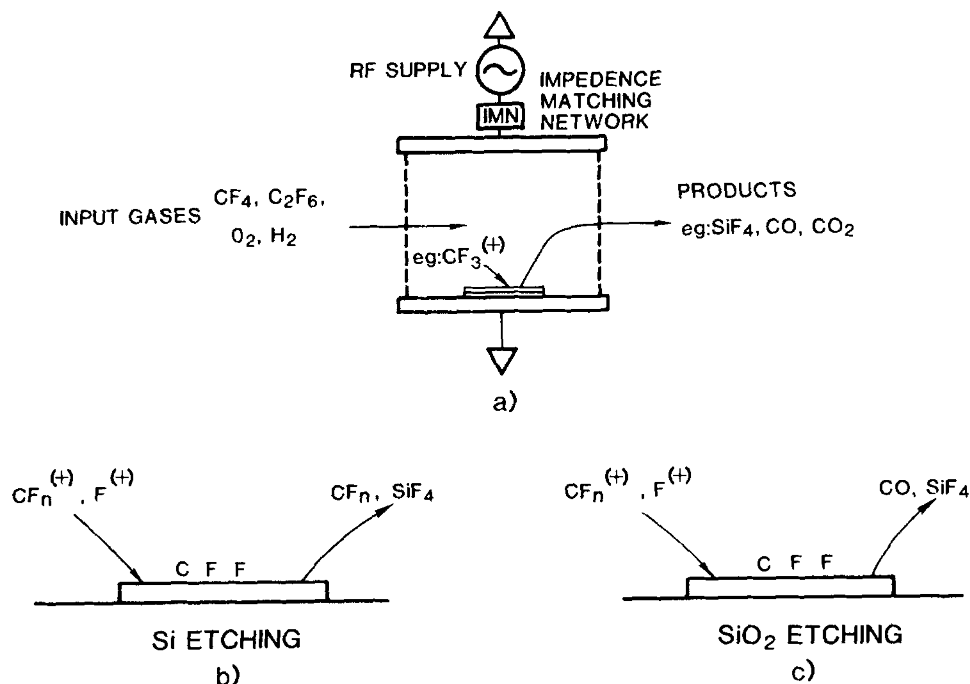

FIG. 1. Schematic of the plasma-etching process. (a) The rf discharge reactor consists of parallel circular electrodes ($\approx$40–50 cm diameter) separated by a few centimeters (<10 cm). The wafer to be etched is placed on the lower electrode. An impedance-matching network is used to maximize power deposited in the reactor. The input gases are fed into the reactor at rates of 10–1000 sccm and products are pumped away. The operating pressure is $\lesssim 100$ mTorr. (b) When etching Si, $CF_n^{(+)}$ and $F^{(+)}$ are adsorbed on the wafer surface, carbon is desorbed as a CF_n molecule, and Si is removed as the desorption product SiF_4. (c) When etching SiO_2, O is removed as the desorption product CO.

Downloaded 27 Mar 2003 to 128.174.115.149. Redistribution subject to AIP license or copyright, see http://ojps.aip.org/japo/japcr.jsp

In the discussion which follows, the input gases are restricted to CF_4, C_2F_6, H_2, and O_2. The transport coefficients and electron-impact cross sections for H_2 and O_2 are well-known.[25] Transport coefficients for CF_4 and C_2F_6 were approximated from their values as a function of E/P.[26] The electron-impact cross sections for CF_4 and C_2F_6, as well as the radicals which are dissociation products, were, with few exceptions, estimates. Among the cross sections which have been measured are those for dissociative attachment.[27,28] Dissociation and ionization cross sections were assumed to have typical threshold behavior so that standard approximate forms could be used.[29,30] The ionization potentials and bond energies can be derived from the appearance potentials of successively smaller ion fragments from the parent molecule.[31]

Vibrational excitation by electron impact is considered in both calculating the electron distribution and in calculating the energy balance in the discharge. The latter is necessary in establishing the steady-state electron density (see below). The vibrational-excitation-impact cross sections for CF_4 and C_2F_6 were calculated by using a Born approximation.[32] The matrix element for the dipole moment of the transition, necessary for the calculation, can be obtained from infrared absorption spectra.[33,34]

Due to the high electron temperature, electron-ion recombination (i.e., radiative and collisional radiative) is not important. Positive and negative ions recombine mainly by diffusion and recombination at the walls and by positive-, negative-ion neutralization. The ion-ion neutralization rate is large, being on the order of 10^{-7} cm^3/s and can be calculated using the method detailed in Ref. 35 by first knowing the ionization potential and electron affinity of the ions.

Neutral- and ion-diffusion coefficients were calculated from the Lennard-Jones radii of the species.[36] Ion diffusion was assumed to be ambipolar so that the diffusion flux of negative ions and electrons is equal to the diffusion flux of positive ions. In this manner, the magnitude of the space-charge field can be solved for and included in the diffusion and etching rates. The local space-charge field is given by

$$\mathscr{E} = \frac{-\sum_i D_i^+ \nabla n_i^+ + \sum_j D_j^- \nabla n_j^-}{\sum_i \mu_i^+ n_i^+ + \sum_j \mu_j^- n_j^-}, \qquad (1)$$

where D_i is the diffusion constant for species i, μ_i is the mobility of species i, and n_i the density of species i. The superscript denotes positive and negative charge carriers.

A summary of the electron-impact events and ion reactions are listed in Table II. In addition to those reactions in Table II, various vibrational- and electronic-excitation reactions for the input gases were included in the Boltzmann calculation.

In the absence of additives, the neutral gas-phase chemistry in CF_4 plasmas is dominated by the reassociation of CF_n radicals with fluorine atoms, and the bi- and termolecular reactions which form C_2F_2, C_2F_4, and C_2F_6. An abbreviated reaction chain for CF_4 plasmas is shown in Fig. 2. There are no stable excited states of CF_4 so electronic excitation is dissociative.[21] This includes the dissociative attachment process forming CF_3^-.[27] Similarly, CF_4^+ has not been observed. The dissociative nature of the CF_4 excited states most likely accounts for the ease in which free fluorine can be produced in these plasmas. (The CF_3-F bond energy is 5.6 eV.) Once CF_3 is produced, CF_2 rapidly follows since the CF_2-F bond

TABLE II. Electron impact collisions and ion reactions.

$e + CF_4 \to CF_3 + F + e$	$e + C_2F_6 \to 2CF_3 + e$
$\to CF_3^+ + F + 2e$	$\to CF_3^- + CF_3$
$\to CF_3^- + F$	$\to CF_3^+ + CF_3 + 2e$
$\to CF_3 + F^-$	$e + C_2F_4 \to 2CF_2 + e$
$\to CF_2 + F + F^-$	$e + C_2F_2 \to 2CF + e$
	$e + SiF_4 \to SiF_3 + F + e$
$e + CF_3 \to CF_2 + F + e$	$e + CHF_3 \to CF_3 + H + e$
$\to CF_3^+ + 2e$	
$\to CF_2^+ + F + 2e$	$e + H_2 \to 2H + e$
$\to CF_2 + F^-$	$\to H_2^+ + 2e$
$\to CF_3^-$	$e + H \to H^+ + 2e$
$e + CF_2 \to CF + F + e$	$e + F \to F^+ + 2e$
$\to CF_2^+ + 2e$	$e + F \to F^-$
$\to CF + F^-$	$e + F_2 \to 2F + e$
	$\to F^- + F$
$e + CF \to C + F + e$	$e + O_2 \to 2O + e$
$\to CF^+ + 2e$	$\to O + O^+ + 2e$
	$\to O_2^+ + 2e$
$e + N^- \to N + 2e$	$\to O + O^-$
$e + P^+ \to P$	
$e + e + P^+ \to e + P$	$e + O \to O^+ + 2e$
	$\to O^-$
$N^- + P^+ \to P + M$	$O^+ + O + M \to O_2^+ + M$
	$H^+ + H + M \to H_2^+ + M$

Note: N^- is any negative ion, P^+ is any positive ion, and M is a third body.

Downloaded 27 Mar 2003 to 128.174.115.149. Redistribution subject to AIP license or copyright, see http://ojps.aip.org/japo/japcr.jsp

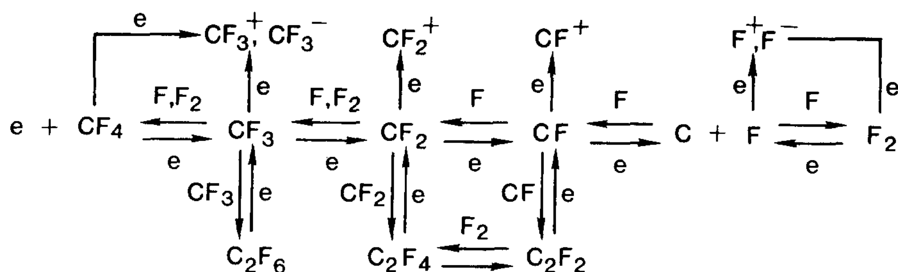

FIG. 2. An abbreviated reaction scheme illustrating electron-impact events and neutral gas-phase reactions in CF_4 and C_2F_6 plasmas.

energy is only 2.2 eV. The CF-F and C-F bond energies are 6.1 and 5.2 eV, so their expected lifetimes are long compared to CF_3. Therefore despite the fact that CF_3 is the first radical to be produced, it may not be the most abundant. The recombinations of CF_3, CF_2, and CF to make C_2F_6, C_2F_4, and C_2F_2, respectively, have large ΔH of formation. Therefore these molecules would appear to be a large reservoir in which CF_n radicals are stored. However, the CF_3-CF_3 bond energy is 4.4 eV, while the CF_2-CF_2 bond energy is 3.3 eV, so electron impact dissociation may also be expected to be large. The reassociation reactions $CF_m + F + M \rightarrow CF_{m+1} + M$ ($m = 0,1,2,3$) are all exothermic; however, they also require a third body (M). Due to the low operating pressure ($\leqslant 100$ mTorr) the termolecular reassociation rate is small. Therefore diffusion and recombination at the walls is the dominant reassociation mechanism.

The reaction chain for C_2F_6 plasmas differs from the CF_4 reaction chain only in the absence of the initiating step involving CF_4. The crucial difference, though, is that a CF_n radical can be produced in the C_2F_6 plasma without liberating any free fluorine. Therefore the *radical* C/F ratio is intrinsically larger in the C_2F_6 plasma. The CF_3-CF_3 bond energy is 4.4 eV, whereas the C_2F_5-F bond energy is 5.5 eV. Therefore the electron-impact dissociation event which produces CF_3 and maintains the larger C/F ratio is more likely than the dissociation which decreases the C/F ratio.

When H_2 or O_2 are added to CF_4 or C_2F_6 discharges, the reaction chain increases in complexity. In a C_nF_m/H_2 discharge, the reaction of CF_l and F with H_2 and H to form HF and CF_3H are the dominant neutral reactions. All of these reactions increase the radical C/F ratio. An abbreviated reaction chain for the CF_4/H_2 system is shown in Fig. 3. The dominant electron-impact events, in addition to those described above, are the dissociation and ionization of H_2

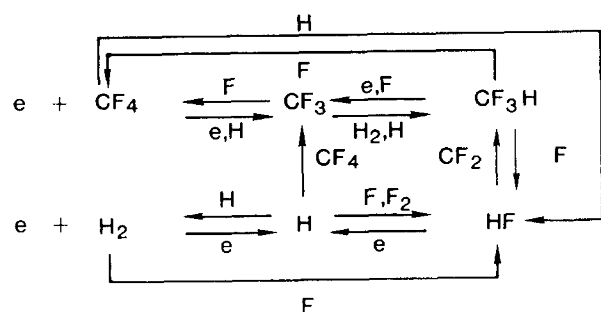

FIG. 3. An abbreviated reaction scheme illustrating additional gas-phase reactions which occur when H is added to CF_4 plasmas.

and the dissociation of CF_3H. Trifluoromethane, CF_3H, is a minor species as compared to HF. The formation of CF_3H could be a reservoir of CF_3 radicals which binds up the adsorbable species. However, the reactions

$$CHF_3 + F \rightarrow CF_4 + H, \quad (2)$$

$$CHF_3 + F \rightarrow CF_3 + HF \quad (3)$$

are relatively fast. The CF_3-H bond energy (4.6 eV) is not large so that electron-impact dissociation is likely. Therefore in the plasma, the CHF_3 density should not be expected to be large. The addition of H_2 also introduces the possibility of adsorption of atomic hydrogen on the surface and subsequent desorption as HF. This effect will be discussed below.

The results of adding oxygen to CF_4 or C_2F_6 discharges are less predictable. Adding oxygen to the discharge increases both the silicon etch rate as well as the fluorescence from excited fluorine atoms.[9,14] This suggests a decrease in the radical C/F ratio by increasing the fluorine atom density. One also has the possibility of adsorbing atomic oxygen on the surface bonding with adsorbed carbon, desorbing as CO. This effect will be discussed below. There are a number of mechanisms proposed to explain the increase in fluorine density which is thought to occur when oxygen is added. The most probable mechanisms involve intermediate species which produce F atoms rather than by a direct method.[9] The first involves OF in the sequence

$$CF_3 + O_2 \rightarrow COF_2 + OF, \quad (4)$$

$$CF_3 + OF \rightarrow COF_2 + 2F, \quad (5)$$

$$OF + OF \rightarrow O_2 + 2F. \quad (6)$$

An alternate scheme involves CF_3O_2:

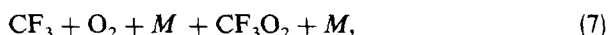

$$CF_3 + O_2 + M + CF_3O_2 + M, \quad (7)$$

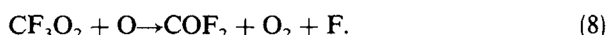

$$CF_3O_2 + O \rightarrow COF_2 + O_2 + F. \quad (8)$$

The initial reaction (4) is exothermic by -14.56 kcal/mole. The analogous reaction with CF_2 is endothermic by 28.5 kcal/mole. The F atom-producing reaction (5) is exothermic by -28.3 kcal/mole, while the analogous reactions with CF_2 and CF are exothermic by -116.4 and -109.0 kcal-/mole, respectively. The net result is that two F atoms are produced by the two-step sequence which consumes two CF_3 molecules. That is, a total of four F atoms result from two electron-impact dissociations of CF_4 to CF_3.

The neutral gas-phase reactions included in the model are listed in Tables III, IV, and V. Table III contains reactions for the CF_4 and C_2F_6 system, Table IV for the C_nF_m/H_2 system, and Table V the C_nF_m/O_2 sytem. When etching SiO_2, oxygen enters the plasma as a desorption prod-

Downloaded 27 Mar 2003 to 128.174.115.149. Redistribution subject to AIP license or copyright, see http://ojps.aip.org/japo/japcr.jsp

TABLE III. Neutral gas phase reactions for etching Si in CF_4 and C_2F_6 plasmas.

Reaction	Reference
$CF_3 + F + M \rightleftharpoons CF_4 + M$	40
$CF_2 + F + M \rightleftharpoons CF_3 + M$	40
$CF + F + M \rightleftharpoons CF_2 + M$	41
$C + F + M \rightleftharpoons CF + M$	a
$CF_3 + F_2 \rightleftharpoons CF_4 + F$	40
$CF_2 + F_2 \rightleftharpoons CF_3 + F$	40
$2CF_3 \rightleftharpoons C_2F_6$	42,43
$2CF_3 + M \rightleftharpoons C_2F_6 + M$	40
$2CF_2 \rightleftharpoons C_2F_4$	44
$2CF_2 + M \rightleftharpoons C_2F_4 + M$	a
$2CF + M \rightleftharpoons C_2F_2 + M$	a
$C_2F_2 + F_2 + M \rightleftharpoons C_2F_4 + M$	a
$F + F + M \rightleftharpoons F_2 + M$	45,46
$SiF_3 + F + M \rightleftharpoons SiF_4 + M$	a
$SiF_2 + F + M \rightleftharpoons SiF_3 + M$	a
$SiF + F + M \rightleftharpoons SiF_2 + M$	a
$SiF_3 + F_2 \rightleftharpoons SiF_4 + F$	a
$SiF_2 + F_2 \rightleftharpoons SiF_3 + F$	a

[a]Rate was estimated.

uct in the form of CO, CO_2, OF, or COF_2. In the pressure of hydrogen, additional O-H reactions are possible. These are listed in Table V. The rate constants for many of the reactions are tabulated in the references indicated. Where the rate constants were not available, they were estimated using standard methods.[37] In the case of hydrogen-transfer reactions, activation energies could be estimated from bond energies.[38] Reverse reaction rates were calculated using the standard equilibrium relationships[37,39]

$$k_r = k_f e^{-(\Delta S/R - \Delta H/RT_g)}, \tag{9}$$

where k_r is the rate constant for the reverse reaction, k_f is the rate constant for the forward reaction, R is the universal gas constant, T_g is the gas temperature, and ΔS and ΔH are the change in entropy and enthalpy, respectively, in going from reactants to products. The forward rate constant is given by

$$k_f = AT^n e^{-E_a/RT_g}, \tag{10}$$

where A is the Arrhenius factor and E_a is the activation energy.

The model for the actual etching process is illustrated in Fig. 1. Neutral- and charged-radical densities produced in

TABLE IV. Additional reactions for C_nF_m/H_2 plasmas.

Reaction	Reference
$CF_4 + H \rightleftharpoons CF_3 + HF$	47
$CF_3 + H \rightleftharpoons CF_2 + HF$	a
$CF_3 + H_2 \rightleftharpoons CHF_3 + H$	48
$CF_2 + HF + M \rightleftharpoons CHF_3 + M$	a
$CHF_3 + F \rightleftharpoons CF_3 + HF$	38
$CHF_3 + F \rightleftharpoons CF_4 + H$	a
$CF_3 + H + M \rightleftharpoons CHF_3 + M$	49
$H + F_2 \rightleftharpoons HF + F$	45,50
$F + H_2 \rightleftharpoons HF + H$	45,50
$H + H + M \rightleftharpoons H_2 + M$	45
$H + F + M \rightleftharpoons HF + M$	45

[a]Rate was estimated.

TABLE V. Additional reactions for C_nF_m/O_2 plasmas.

Reaction	Ref.	Reaction	Ref.
$CF_3 + O_2 \rightleftharpoons COF_2 + FO$	a	$CO_2 + O \rightleftharpoons CO + O_2$	53,54
$CF_2 + O_2 \rightleftharpoons COF + FO$	a	$C_2F_4 + O \rightleftharpoons COF_2 + CF_2$	57
$CF_3 + FO \rightleftharpoons COF + 2F$	a	$O + H + M \rightleftharpoons OH + M$	a
$CF_2 + FO \rightleftharpoons COF + F$	a	$O + H_2 \rightleftharpoons H + OH$	53,56
$CF + FO \rightleftharpoons COF + F$	a	$O + OH \rightleftharpoons O_2 + H$	58
$FO + FO \rightleftharpoons O_2 + 2F$	52	$OH + H_2 \rightleftharpoons H_2O + H$	56
$O + F + M \rightleftharpoons FO + M$	a	$OH + H + M \rightleftharpoons H_2O + M$	56
$O + FO \rightleftharpoons O_2 + F$	a	$2OH \rightleftharpoons H_2O + O$	53,56
$C + O + M \rightleftharpoons CO + M$	53,54	$CO_2 + H \rightleftharpoons OH + CO$	56,59
$O + O + M \rightleftharpoons O_2 + M$	53,55	$CO_2 + H_2 \rightleftharpoons CO + H_2O$	53
$CO + O + M \rightleftharpoons CO_2 + M$	56	$F + OH \rightleftharpoons HF + O$	45
$CO + F + M \rightleftharpoons COF + M$	a	$F + H_2O \rightleftharpoons HF + OH$	45
$COF + F + M \rightleftharpoons COF_2 + M$	a	$F_2 + OH \rightleftharpoons O + HF + F$	45

[a]Rate was estimated.

the volume diffuse (either by neutral- or space-charge-enhanced diffusion) to the substrate surface. A fraction γ of these radicals are adsorbed while the rest return to the plasma. The radicals which can be adsorbed were assumed to be $CF_3^{(\pm)}$, $CF_2^{(+)}$, $CF^{(+)}$, C, $F^{(\pm)}$, $O^{(\pm)}$, and $H^{(+)}$, where the superscript denotes that both neutral and charged species are included. No distinction is made between the neutral and charged species in the adsorption process, as it was assumed that the charged radicals are neutralized on or near the surface prior to adsorption. The ambipolar diffusion flux therefore represents a mechanism which can efficiently transport radicals to the surface. For a given density, ions can therefore have a higher flux to the surface than neutrals.

For etching silicon dioxide, it was assumed that the desorption product which removes the oxygen is carbon monoxide (CO). Therefore, for every SiO_2 molecule removed, two carbon atoms must be adsorbed. Concurrently, at least four fluorine atoms must be adsorbed in order to remove the silicon atom as the desorption product SiF_4. The SiO_2 etch rate (μm/min) is therefore the smaller of

$$\mathscr{R}^E_{SiO_2} = \frac{mh\gamma}{2\rho\Lambda^2}\left[\sum_{n=0}^{3}([CF_n]D_n + [CF_n^{(\pm)}]D_n^a) - (1-\alpha_O)([O]D_O + [O^+]D_O^a)\right] \tag{11a}$$

$$\mathscr{R}^E_{SiO_2} = \frac{mh\gamma}{2\rho\Lambda^2}\left[\sum_{n=1}^{3} n([CF_n]D_n + [CF_n^{(\pm)}]D_n^a + [F]D_F + [F^{(\pm)}]D_F^a - (1-\alpha_H) \times([H]D_H + [H^+]D_H^a)\right], \tag{11b}$$

where $[x]$ is the density of species x, D_n is the diffusion coefficient of a neutral species, D_n^a is the ambipolar diffusion constant of a charged species, Λ is the diffusion length of the reactor, h is the height of the reactor, m is the molecular weight of SiO_2, ρ is the mass density of SiO_2, and γ is the adsorption probability. The terms containing [O] and [H] will be discussed below. Equation (11a) is the rate-limiting expression for desorbing the oxygen while equation (11b) is the rate-limiting step for desorbing the silicon.

Downloaded 27 Mar 2003 to 128.174.115.149. Redistribution subject to AIP license or copyright, see http://ojps.aip.org/japo/japcr.jsp

When etching silicon, it was assumed that the first priority of fluorine atoms which have been adsorbed on the surface is to remove carbon atoms which have also been adsorbed, thereby preventing polymerization. The remaining fluorine removes silicon as the desorption product SiF_4. The major desorption product for carbon was assumed to be CF_4, but in principle could be a CF_n radical. Clearly, some carbon must be desorbed in radical form in order for there to be any fluorine left to etch the silicon. Therefore, the parameter α has been introduced as that fraction of adsorbed carbon which is desorbed as a radical. One can interpret this parameter in terms of the average desorption product being CF_δ, where $\delta = 4(1-\alpha)$. The etching characteristics are a sensitive function of its precise value, and this will be discussed below. The silicon etch rate (μm/min) is therefore

$$\begin{aligned}\mathscr{R}^E_{\rm Si} = \frac{mh\gamma}{4\rho\Lambda^2}\Bigg[& \sum_{n=1}^{3} n([{\rm CF}_n]D_n + [{\rm CF}_n^{(\pm)}]D_n^a) \\ & -(1-\alpha_{\rm H})([H]D_{\rm H} + [{\rm H}^+]D_{\rm H}^+) + [{\rm F}]D_{\rm F} \\ & + [{\rm F}^{(\pm)}]D_{\rm F}^a - 4(1-\alpha)\Bigg[\sum_{n=0}^{3}([{\rm CF}_n]D_n \\ & + [{\rm CF}_n^{(\pm)}]D_n^a) - (1-\alpha_{\rm O})([{\rm O}]D_{\rm O} + [{\rm O}^+]D_{\rm O}^a)\Bigg]\Bigg], \end{aligned} \tag{12}$$

where now m and ρ refer to the molecular weight and density of silicon. Note that for sufficiently high radical C/F ratios, $\mathscr{R}^E_{\rm Si}$ can be negative. A negative value of $\mathscr{R}^E_{\rm Si}$ means that carbon is being removed at a slower rate than it is being adsorbed; that is, polymerization on the semiconductor surface is taking place. The terms containing [O] and [H] will be discussed below.

The adsorption probability for CF_n radicals on clean silicon has been measured to be between 0.08 and 0.75, while the dissociative adsorption to CF_4 has a probability of less than 10^{-7}.[17] Therefore the adsorption probability γ was assumed to be 0.5 on both Si and SiO_2 for all radicals, while saturated molecules are not adsorbed.

In mixtures of C_nF_m with O_2 and H_2, adsorption of atomic oxygen and hydrogen may also occur. These adsorbed atoms may then react with an adsorbed fluorine or carbon atom, desorbing as HF or CO. In the case of etching in C_nF_m/H_2 mixtures, adsorbed hydrogen which consumes an adsorbed fluorine atom in forming HF will promote polymerization on silicon surfaces. This is due to the requirement that carbon be desorbed as a CF_n radical or molecule. Desorption of HF decreases the available F atoms for both etching and removal of carbon. Oxide etch rates may also be reduced if the HF desorption process consumes enough fluorine on the surface so that the removal of Si by the desorption of SiF_4 becomes the rate-limiting step. In C_nF_m/O_2 mixtures, the adsorption of oxygen on silicon which is desorbed as CO cleanses the surface and delays polymerization by removing carbon. In etching the oxide, adsorption of oxygen and the desorption of CO is detrimental to the etching process as adsorbed carbon is necessary to remove lattice oxygen.

The effect of oxygen and hydrogen adsorption on the computed etch rates is included in the following manner. In the case of adsorbed oxygen, the density of adsorbed carbon on the surface is reduced by the rate at which oxygen is adsorbed and desorbed as CO. In the case of adsorbed hydrogen, the density of adsorbed fluorine on the surface is reduced by the rate at which hydrogen is adsorbed and desorbed as HF. These terms are included in expressions (11) and (12). The effect of these processes on computed etch rates can be large.

The effect of the continuous stream of input gases and pumping away of products has been put in the model by including in the expression for the time derivative of the density of species x_j the partial derivative

$$\frac{\partial [x_j]}{\partial t} = \frac{f\mathscr{L}}{\pi R^2 h}\left[M_j - \frac{[x]_j}{\sum_j [x]_j}\right], \tag{13}$$

where f is the total input flow rate in scc/sec, $\mathscr{L}$ is Loschmidt's number, R is the radius of the reactor and M_j is the mole fraction of species j in the input gas stream. The first term represents the increase in $[x_j]$ due to the input gas stream, while the second term represents the decrease $[x_j]$ due to pumping away the products.

In a plasma-etching reactor setup, there is usually an impedance-matching network between the rf amplifier and the actual reactor. It can be shown that the maximum power is coupled into the reactor when the impedance of the network and reactor is equal to the output impedance of the rf amplifier.[2] Assuming a small fraction of this energy is dissipated in the network, then the average voltage seen by the reactor is simply

$$\bar{V} = (PR_0)^{1/2}, \tag{14}$$

where P is the power deposited in the gas and R_0 is the output impedance of the amplifier. This value of $\bar{V}$ is used to calculate the average electric field required for the Boltzmann calculation. The average electron density is also determined by the power deposited in the gas:

$$n_e = \frac{P}{\pi R^2 h \sum_j r_j^\epsilon [x_j]}, \tag{15}$$

where n_e is the electron density and r_j^ϵ is the rate at which electrons lose energy to species j per unit volume.

Rate equations were formed including all the processes discussed above. The electron-impact rates are first obtained by solving for the electron-distribution function, and then the rate equations are integrated until a steady-state solution is obtained. The steady-state solution was determined by when the densities of the major species (e.g., CF_4, CF_3, CF_2, F) did not change by more than a few parts in a thousand over a period which was many times longer than the time required for neutral species to diffuse to the surface. The final densities and fluxes are then used to calculate the steady-state plasma-etching rate. Results from the calculation are discussed below.

III. RESULTS FROM THE SIMULATION OF rf PLASMA ETCHING IN C_nF_m/H_2 GAS MIXTURES

One of the most desirable attributes of plasma etching would be the ability to etch a contact window through an

Downloaded 27 Mar 2003 to 128.174.115.149. Redistribution subject to AIP license or copyright, see http://ojps.aip.org/japo/japcr.jsp

oxide layer to the silicon layer below with infinite selectivity. As was discussed previously, the addition of H_2 to CF_4 and C_2F_6 increases the rate at which SiO_2 is etched with respect to Si by binding up free fluorine, principally in the form of HF, and by the possible adsorption of atomic hydrogen on the semiconductor surface. Typical experimental results for etching Si and SiO_2 in CF_4/H_2 mixtures are shown in Fig. 4. Etch rates computed with the model for similar conditions are shown in Fig. 5. The systematic agreement with experimental is good as the increase in selectivity of SiO_2 with respect fo Si is clearly indicated in the calculation. The principle product of the gas-phase chemistry is HF. The abundance of CF_3H is orders of magnitude smaller (see Fig. 6). The increase in selectivity of SiO_2 with respect to Si is confirmed to be a result of the decrease in free fluorine due to the formation of HF and the increase in the radical C/F ratio as a result of reaction such as

$$CF_3 + H \rightarrow CF_2 + HF. \quad (16)$$

The fractional contribution of ions to the etching process is 0.6–0.65 for Si and 0.7–0.8 for SiO_2 over the range of CF_4/H_2 ratios, even though the ion density is 3–4 orders of magnitude smaller than the neutral density (see Fig. 6). The ion contribution remains high as the CF_4/H_2 ratio decreases, a result in part due to the efficient conversion of the neutral radicals to HF. The selectivity of etching SiO_2 with respect to Si calculated by the model is shown in Fig. 7, where we also see the increased selectivity of C_2F_6/H_2 mixtures as compared to CF_4/H_2 mixtures. The increase in selectivity is due to the increase in the average radical C/F ratio.

The most abundant radicals in the discharge are CF_2 and CF, not CF_3 as one might expect. The longevity of the CF_2 radical is mentioned by Flamm[5] and Truesdale.[10] Experimental verification of the abundance of a radical such as CF_n by mass spectroscopy is difficult. The probes are usually downstream of the discharge so that there is a transit time between radicals leaving the discharge and detection by the probes. Therefore reassociation reactions such as

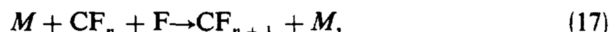

$$M + CF_n + F \rightarrow CF_{n+1} + M, \quad (17)$$

$$CF_n + F_2 \rightarrow CF_{n+1} + F, \quad (18)$$

and diffusion have time to significantly reduce the radical density. The presence of CF_2 and CF radicals in the discharge region have been confirmed by optical spectroscopy.[15,51]

The problem of extrapolating mass spectroscopic measurements made downstream of the discharge to conditions in the discharge is significant. For example, in the mass spectroscopic measurements made by Truesdale,[10] the probe was located 15 cm downstream of the discharge region, requiring a transit time for the species as long as 50 ms. During this time a variety of gas-phase and surface reactions may occur to change the composition of the gas.

To investigate this problem, species densities for conditions similar to Truesdale's[10] experiment have been calculat-

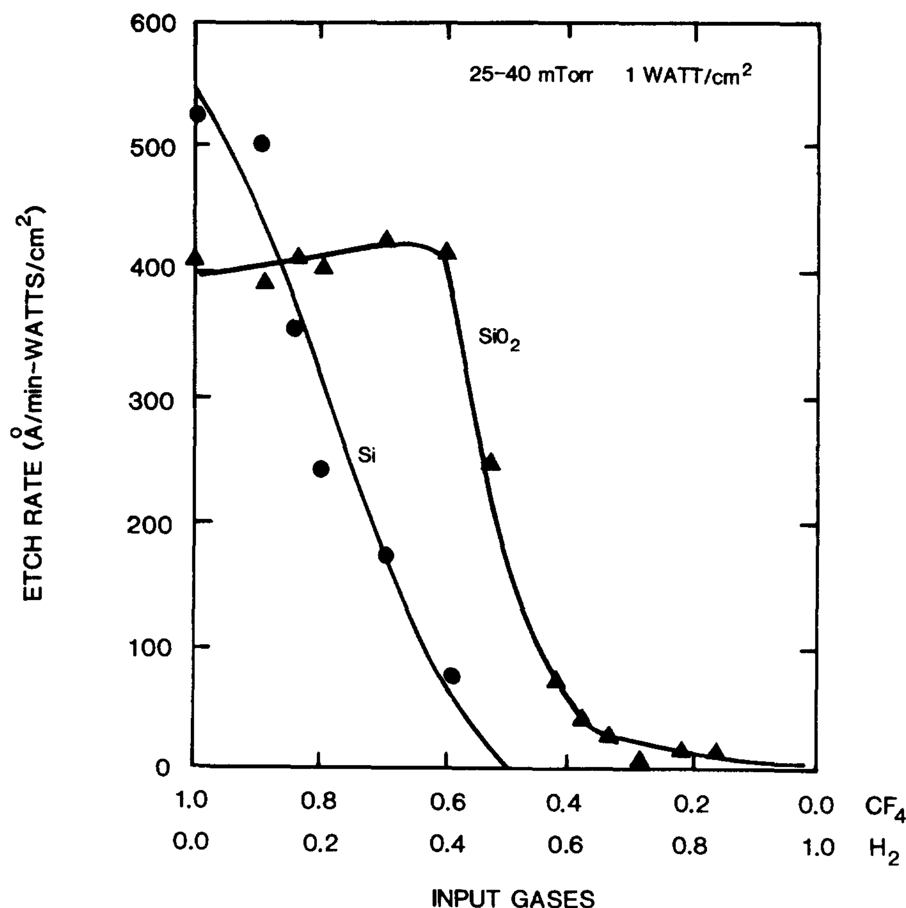

FIG. 4. Typical experimental results for eching Si and SiO_2 in CF_4/H_2 plasmas. (The etch rate has been normalized by the rf discharge power per unit area of the reactor.) Discharge power was 100 W over 100 cm^2 of electrode area and a total pressure of 3–5 Pa (from Ref. 6).

Downloaded 27 Mar 2003 to 128.174.115.149. Redistribution subject to AIP license or copyright, see http://ojps.aip.org/japo/japcr.jsp

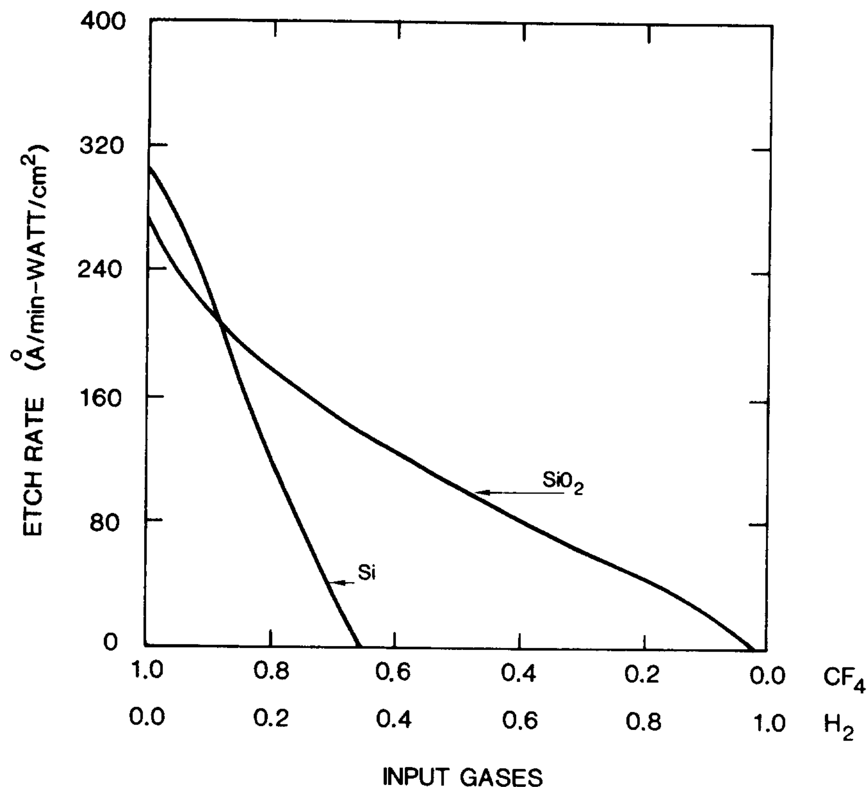

FIG. 5. Computed etch rates of Si and SiO_2 in CF_4/H_2 plasmas. The total pressure was held constant at 100 mTorr and the rf power constant at 0.25 W/cm^2.

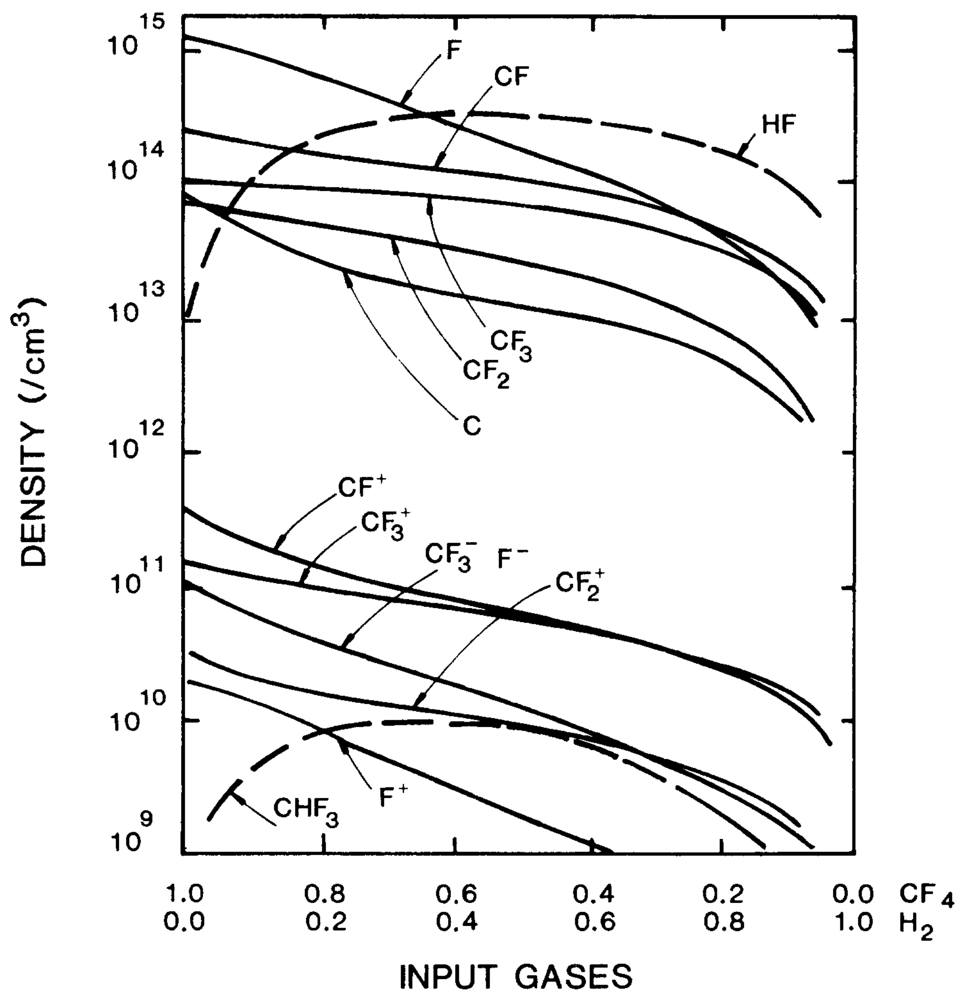

FIG. 6. Radical and ion densities in CF_4/H_2 plasmas computed with the model. For comparison, the densities of product species HF and CF_3H are also plotted. The contribution of neutral radicals and ions to the etching process are nearly equal.

Downloaded 27 Mar 2003 to 128.174.115.149. Redistribution subject to AIP license or copyright, see http://ojps.aip.org/japo/japcr.jsp

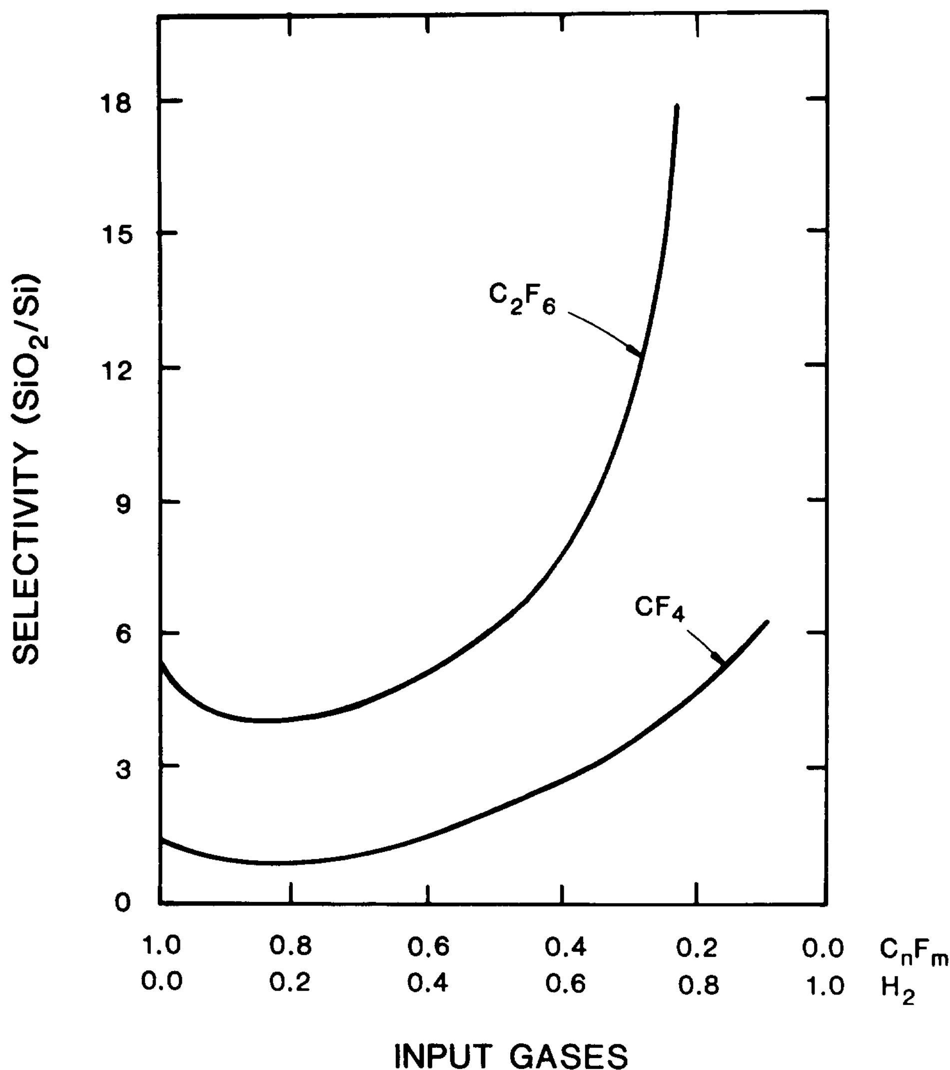

FIG. 7. Selectivity of etching SiO_2 with respect to Si in CF_4/H_2 and C_2F_6/H_2 plasmas computed for identical discharge conditions. The higher selectivity in C_2F_6/H_2 plasmas is due to the larger C/F ratio of the adsorbable species.

ed with the model. In that experiment, a CF_4/H_2 mixture was flowed through a 1.9-cm-i.d. alumina tube. The gas first passed through a 5-cm-long discharge region before flowing an additional 15 cm to a quadrupole mass spectrometer. For a flow rate of 25 sccm at 0.5 Torr pressure, the residence time in the discharge region was 15–20 ms and the transit time to the probe was 45–60 ms. To simulate the experiment, discharge conditions were calculated after which high-threshold electron-impact events (e.g., ionizations and dissociations) were turned off. (No silicon compounds were present.) Densities were computed for an additional 50 ms to simulate the transit time to the probe. These results are shown in Fig. 8 and show excellent agreement with Truesdale's measurements, which are shown in Fig. 9. In Fig. 10, the same quantities are plotted for conditions as the gas leaves the discharge region. Large fractions of CF_3, CF_2, CF, F, and H are present which do not survive to the downstream position. These radicals quickly reassociate. The products of the reassociation are primarily CF_4, C_2F_6, C_2F_2, H_2, and HF. Atomic hydrogen recombines at a somewhat slower rate, although this may be an artifact of the model since hydrocarbon species are not included in the model.

In the balance of forward and backward reactions for the dissociation of molecules and the reassociation of radicals, there is usually only a single characteristic temperature—the gas temperature. In a plasma, the dissociation rate is characterized by the electron temperature ($T_e > 10^4$ K), while the reassociation rate is characterized by the gas temperature ($T_g < 10^3$ K). Since

$$k_d \sim k_r e^{-\Delta H/RT}, \qquad (19)$$

where k_d is the dissociation rate, k_r is the reassociation rate, ΔH is the change in enthalpy and T is the characteristic temperature, when $T = T_e$, k_d, and k_r can be close to the same value in a plasma. As species leave the plasma, the characteristic temperature in (19) changes from T_e to T_g so that $k_d \ll k_r$ and reassociation dominates. It is this transition in temperature which is responsible for the results discussed above.

In a C_nF_m/H_2 discharge, atomic hydrogen may be adsorbed on the semiconductor surface. The specific role of the adsorbed additive can greatly influence the etching process. Consider the adsorption of atomic hydrogen on silicon and its oxide in a CF_4/H_2 plasma. Assume that the adsorbed hydrogen reacts with absorbed fluorine to form HF which is subsequently desorbed back into the plasma. The reaction sequence is

$$H^{(+)}(g) \rightarrow H\,(ads), \qquad (20)$$

Downloaded 27 Mar 2003 to 128.174.115.149. Redistribution subject to AIP license or copyright, see http://ojps.aip.org/japo/japcr.jsp

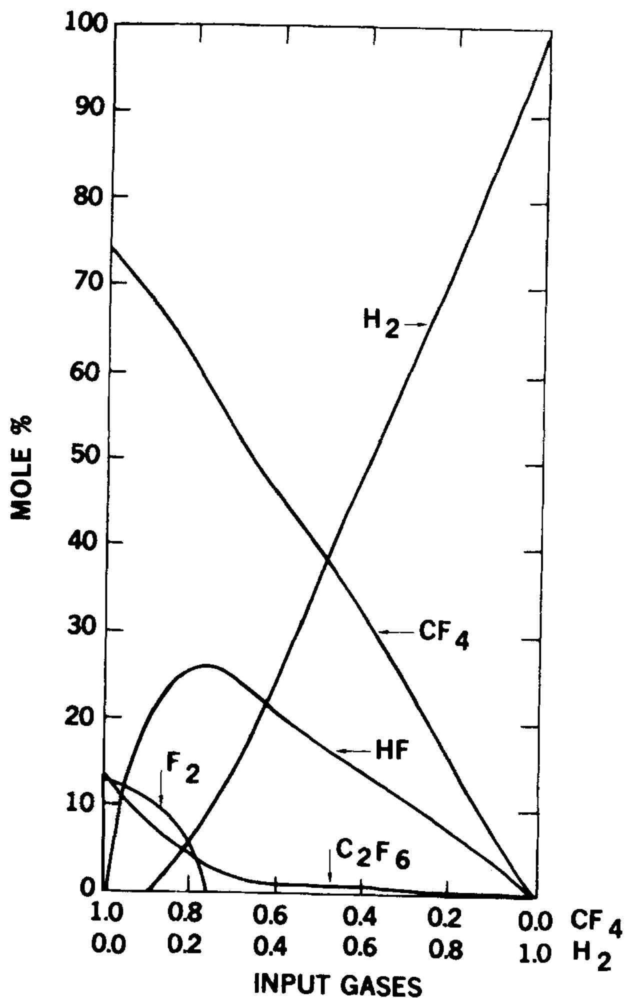

FIG. 8. Computed results for the mole percent of species arriving at a mass spectroscopic probe 15 cm downstream of the discharge region in CF_4/H_2 plasmas. The transit time was ≈ 50 ms. Total pressure was held constant at 0.5 Torr.

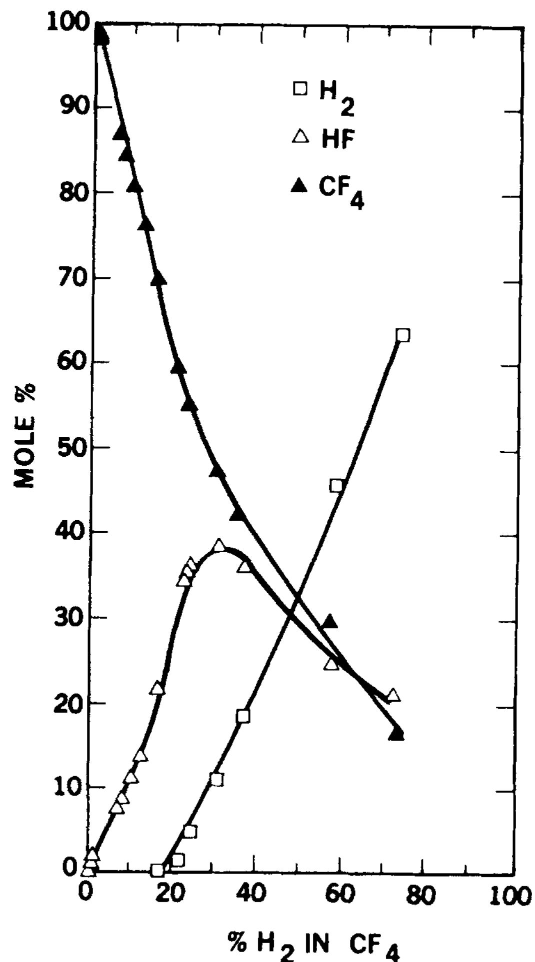

FIG. 9. Experimental results for the conditions described in Fig. 8 (from Ref. 10).

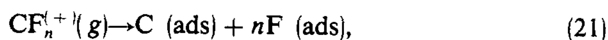

$$CF_n^{(+)}(g) \rightarrow C\ (ads) + nF\ (ads), \tag{21}$$

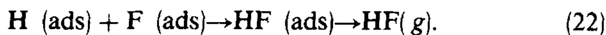

$$H\ (ads) + F\ (ads) \rightarrow HF\ (ads) \rightarrow HF(g). \tag{22}$$

The probability for reaction (22) is $(1 - \alpha_H)$, where α_H is the desorption probability. From Eq. (12) we see that this reaction results in a decrease in the silicon etch rate. The number of fluorine atoms available to combine with adsorbed carbon (to desorb as CF_4) and to combine with silicon (to desorb as SiF_4) is reduced by the formation of HF on the surface. The affect on the etch rate of silicon of the reaction sequence (20)–(22) is illustrated in Fig. 11. Again, the onset of polymerization occurs when the etch rate falls to zero.

Examining the effect of reactions (20)–(22) on the SiO_2 etch rate, we obtain the results in Fig. 12. Recall that the oxide etch rate is limited by the smaller of the two desorption processes which remove oxygen and silicon, respectively. The former requires carbon (desorption product CO), while the latter requires fluorine (desorption product SiF_4). For hydrogen fractions less than 15%, the SiO_2 etch rate is limited by the removal of oxygen so that the rate is insensitive to reaction (22). In the range of 15–25% hydrogen, there is a transition in the rate-limiting step from the removal of oxygen to the removal of silicon, and the etch rate becomes very sensitive to the deprivation of fluorine on the surface. In the instances where half-or-more of the adsorbed hydrogen reacts to form HF, polymerization on the oxide surface is likely to occur.

The most sensitive parameter on which the etch rate of silicon depends is the specific radical (or molecule) by which carbon is desorbed from the surface. In Fig. 13, the etch rate of silicon as a function of α and the CF_4/H_2 ratio is plotted. (Recall that the average carbon desorption product is $CF_{4(1-\alpha)}$.) In the extreme cases where C atoms and CF are the major desorption products ($\alpha \gtrsim 0.75$), little if any polymerization occurs, and the silicon etch rate is always greater than the oxide etch rate. At the other extreme, where the average desorption product is CF_3($\alpha \lesssim 0.4$), the etch rate is never greater than zero and polymerization occurs for all CF_4/H_2 ratios. Based on these results, one can estimate that $0.4 < \alpha < 0.75$ and most likely is nearer 0.5–0.6. This translates to the average desorption product being CF_2.

Downloaded 27 Mar 2003 to 128.174.115.149. Redistribution subject to AIP license or copyright, see http://ojps.aip.org/japo/japcr.jsp

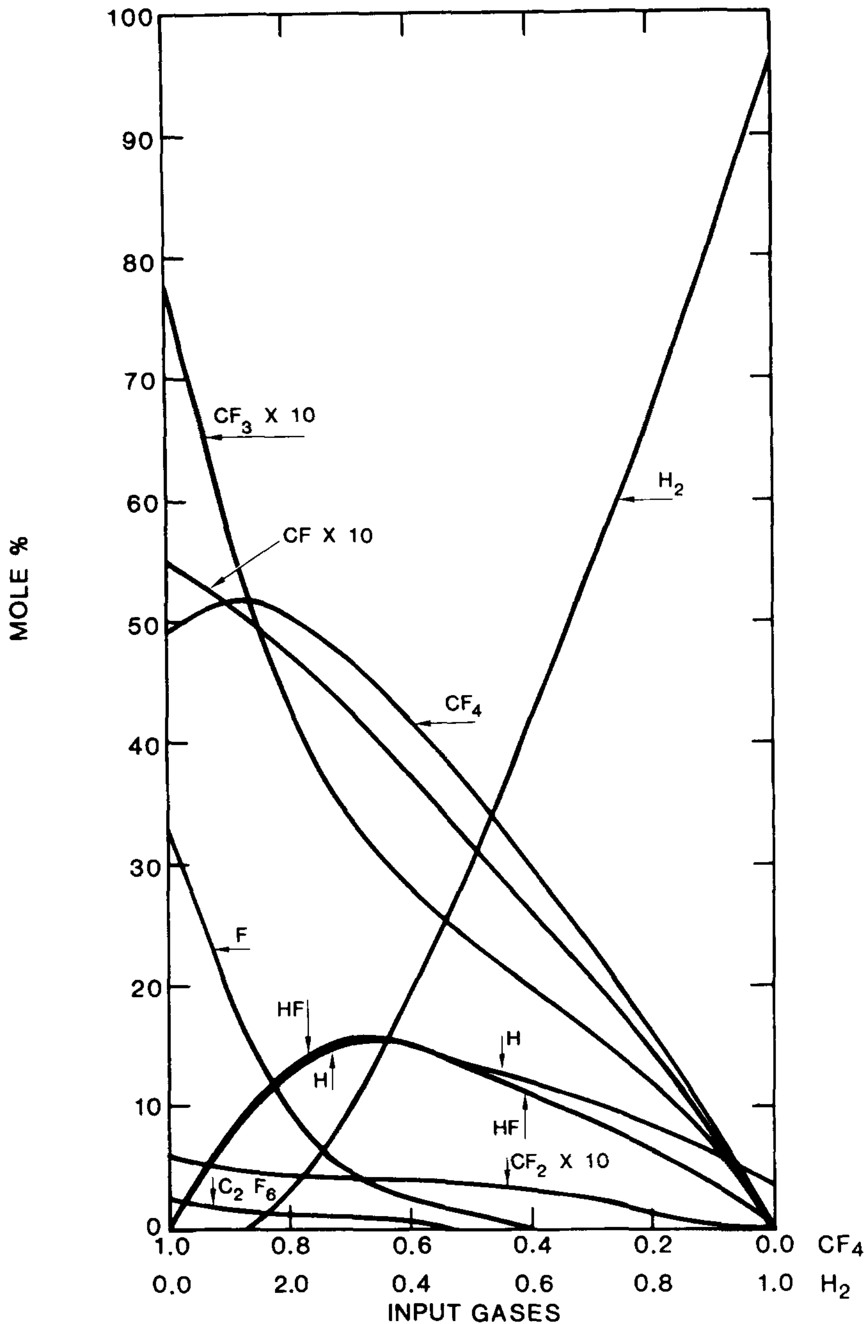

FIG. 10. Mole percent of species emerging from the discharge region for the conditions of Fig. 8 as computed with the model. Virtually all of the radical species recombine before the downstream measurement is made.

IV. RESULTS FROM THE SIMULATION OF rf PLASMA ETCHING IN CF_4/O_2 GAS MIXTURES

It has been proposed that the increase in the etch rate of silicon in C_nF_m/O_2 plasmas is a result of an increase in the free fluorine density due to reactions such as (4)–(8). Typical experimental results for etching Si in CF_4/O_2 plasmas are shown in Fig. 14. The correlation between the increase in silicon etch rates and atomic fluorine density is based on observation of excited-fluorine fluorescence (7904 Å). Although the correlation of excited fluorine with the total fluorine density (and hence silicon etch rate has been made empirically, there are instances where the excited-state density of fluorine can be increased with little change in the etch rate. One such example is the charge-transfer reaction

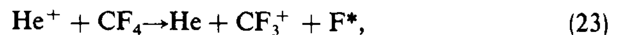

$$He^+ + CF_4 \rightarrow He + CF_3^+ + F^*, \quad (23)$$

which greatly increases the 7904-Å fluorine emission, while making a nominal change in the silicon etch rate.[60]

An alternate explanation has been proposed for the enhancement in the silicon etch rate with added oxygen. This explanation relies in part on the affect of adsorbed atomic oxygen on the silicon surface. This oxygen combines with adsorbed carbon, desorbing as CO. This is a cleansing process which rids the surface of carbon, reduces the probability of polymerization, and leaves more adsorbed fluorine available to etch. The results of this study favor the latter explanation.

The CF_4 molecule does not react with atomic or molecular oxygen[61]; radicals such as CF_3 do. The radical CF_3 is

Downloaded 27 Mar 2003 to 128.174.115.149. Redistribution subject to AIP license or copyright, see http://ojps.aip.org/japo/japcr.jsp

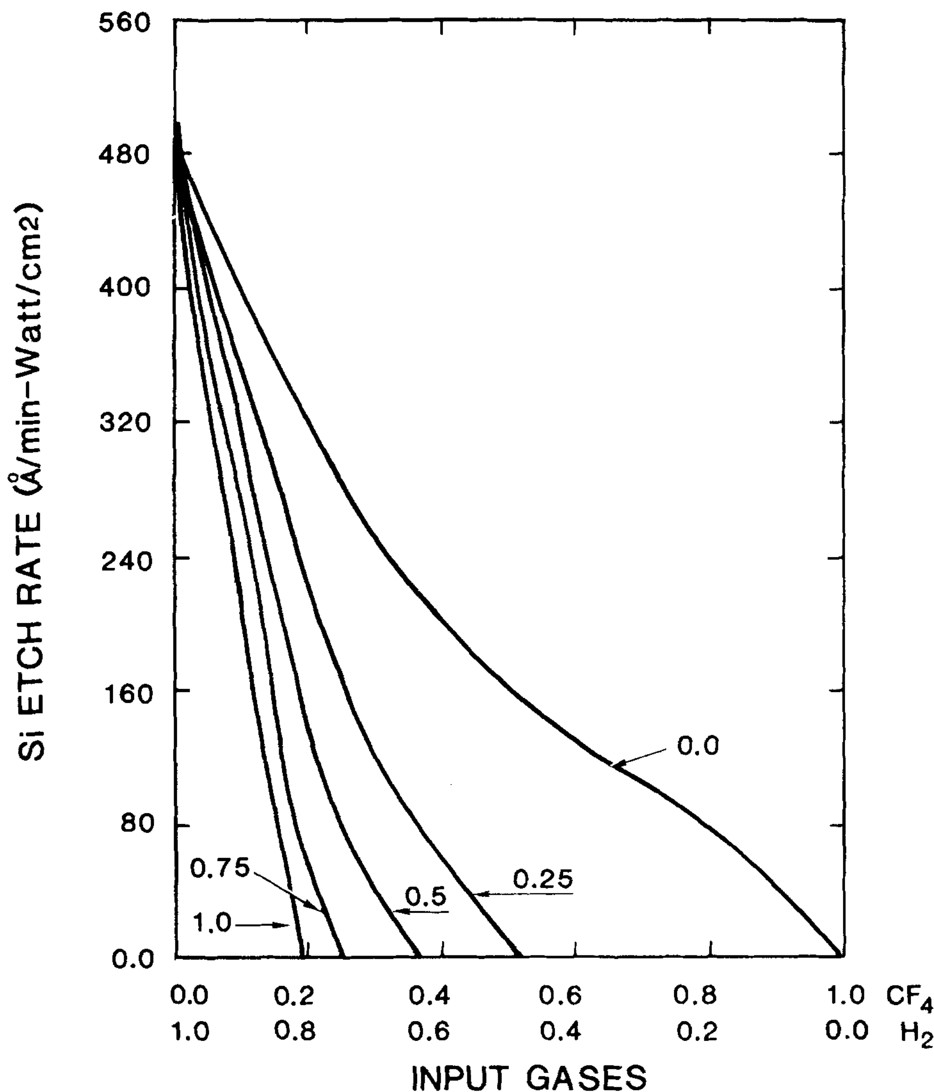

FIG. 11. The dependence of the etch rate of Si on the probability of adsorbed H and F being desorbed from the surface as HF [i.e., reaction (22)]. In the calculation, this probability is $(1-\alpha_H)$, where α_H is the hydrogen desorption probability.

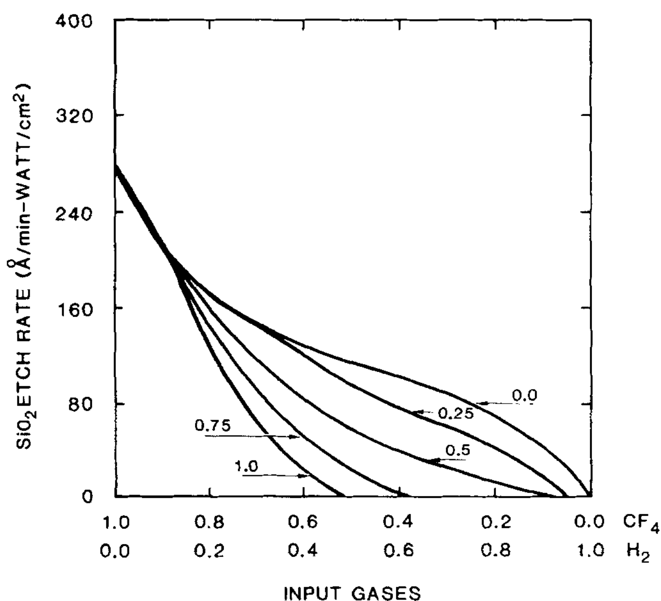

FIG. 12. The dependence of the etch rate of SiO_2 on the probability of adsorbed H and F being desorbed from the surface as HF [i.e., reaction (22)]. In the region between 15 and 25% H_2, the rate-limiting step in the process changes from the removal of O from the surface to the removal of Si from the surface.

adsorbed with high probability on silicon, as is atomic fluorine. Assuming that COF_2 is not adsorbed on silicon, reactions (4) and (5) which yield the net reaction

$$2CF_3 + O_2 \rightarrow 2COF_2 + 2F \quad (24)$$

actually reduces the number of fluorine atoms which can be adsorbed. The advantage of this reaction sequence is that the number of carbon atoms which may also be adsorbed is reduced. If one assumes that the average desorption product is CF_2 (see previous discussion) and the adsorption probability of CF_3 and F are nearly equal, then there is no net benefit to reducing two adsorbable CF_3 radicals to two adsorbable F atoms. In each case, two F atoms are available for etching. Therefore, reactions such as (24) cannot significantly change the silicon etch rate despite an apparent increase in fluorine density. Since the enhancement in silicon etch rates with the addition of oxygen is observed in many gases (CF_4, C_2F_4, C_2F_6), the mechanism should be relatively independent of any specific radical. In addition, the ion contribution to the etch rate is about 0.6, so that enhancements in etch rates by factors of 5–10 must include a mechanism which involves ions or adsorbed ions.

For the reasons cited in the discussion above and the calculated results to be discussed, the adsorption of oxygen

Downloaded 27 Mar 2003 to 128.174.115.149. Redistribution subject to AIP license or copyright, see http://ojps.aip.org/japo/japcr.jsp

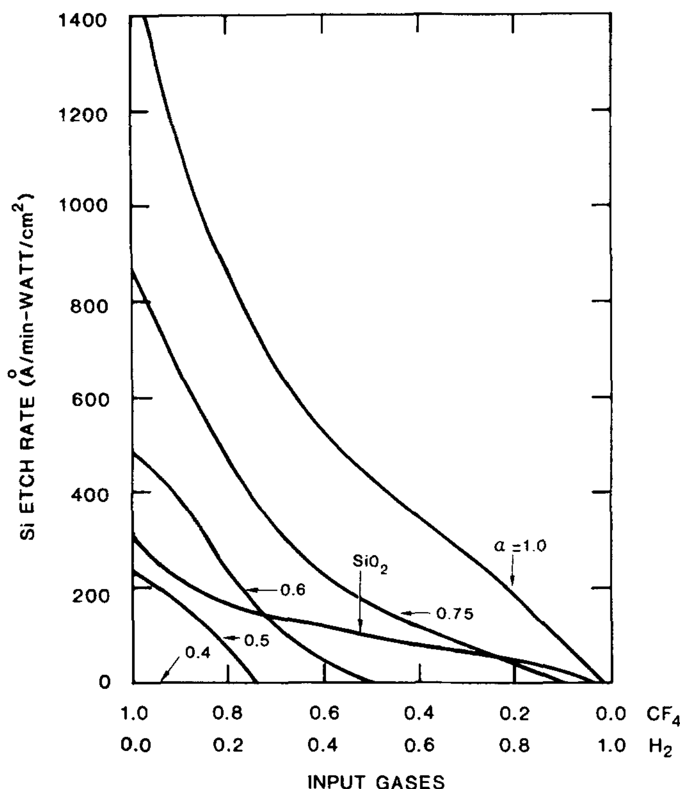

FIG. 13. Si etch rates as a function of the probability of desorption α. The average number of fluorine atoms in the desorption product CF_δ is $\delta = 4(1 - \alpha)$. The oxide etch rate is shown for comparison.

and desorption of CO (cleansing the surface of carbon) is favored as the major mechanism which increases the silicon etch rate. In Fig. 15, calculated etch rates for a discharge in CF_4/O_2 mixtures are plotted as a function of the probability that adsorbed oxygen is desorbed as CO. The increase in the silicon etch rate in the region of 0.2 mole fraction of oxygen is due to the gas-phase reactions discussed above. The relative increase is only 10–15%, far smaller than the factor of 6 enhancement seen experimentally (Fig. 14). This result is not strongly dependent on the estimated rates for reactions (4)–(8). The values of the reaction rates were made as large as was thought reasonable, and no significant increase in etch rates was observed. (The rates were made as large as the exothermic reactions which form HF, i.e., $k \approx 5 \times 10^{12}$ cm^3/mole s.) These results depend on the maximum fractional increase in F density which could occur by reaction (24) if all CF_3 were converted to COF_2, OF, and F. For our conditions, this increase is only a factor of 2.

Note, though, that as the probability for the desorption of CO is increased, the silicon etch rate increases sharply with a maximum coming near a CF_4/O_2 ratio of $\sim 0.2/0.8$. The calculated CF_4/O_2 ratio at which the maximum occurs is larger than is observed experimentally, but the calculation does reproduce the systematic results. In the calculation, the adsorption probability of oxygen atoms was made equal to that of the CF_n radicals and F atoms. By increasing the probability of adsorbing oxygen with respect to the fluorocarbons and fluorine, the maximum in the etch rate can be made to occur at smaller CF_4/O_2 ratios.

There are two processes not included in the calculation which would increase the net fluorine density and contribute to reactions such as (4)–(8) as being the dominant mechanism

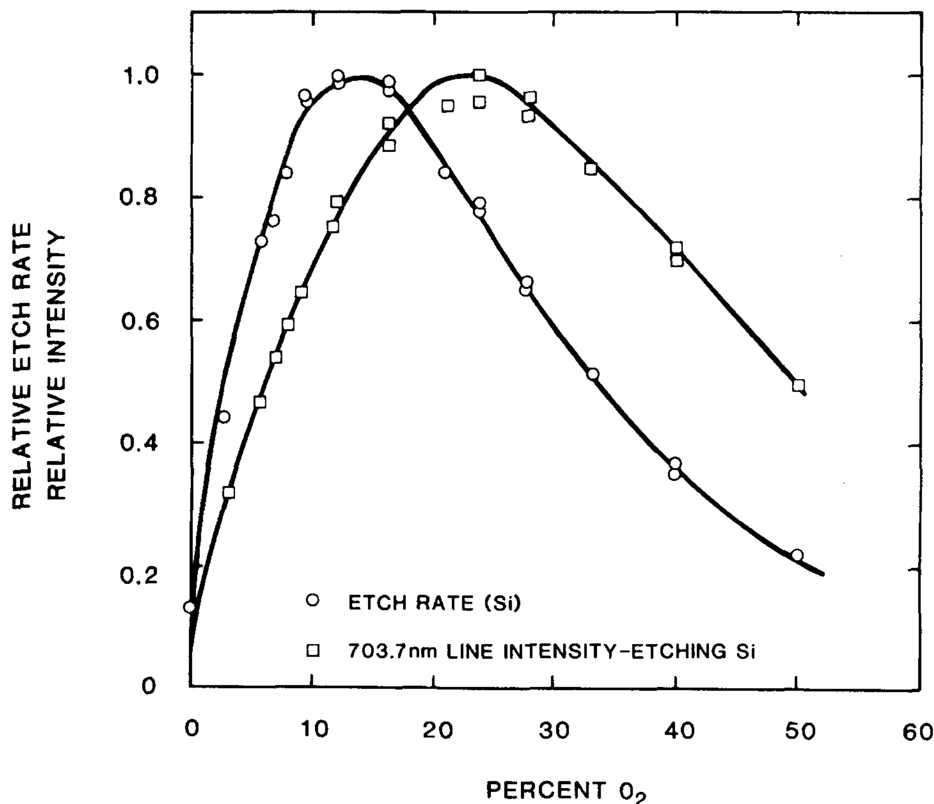

FIG. 14. Typical experimental results for the etching of Si in CF_4/O_2 plasmas and the concurrent intensity of excited fluorine emission (7904 Å) (from Ref. 9).

Downloaded 27 Mar 2003 to 128.174.115.149. Redistribution subject to AIP license or copyright, see http://ojps.aip.org/japo/japcr.jsp

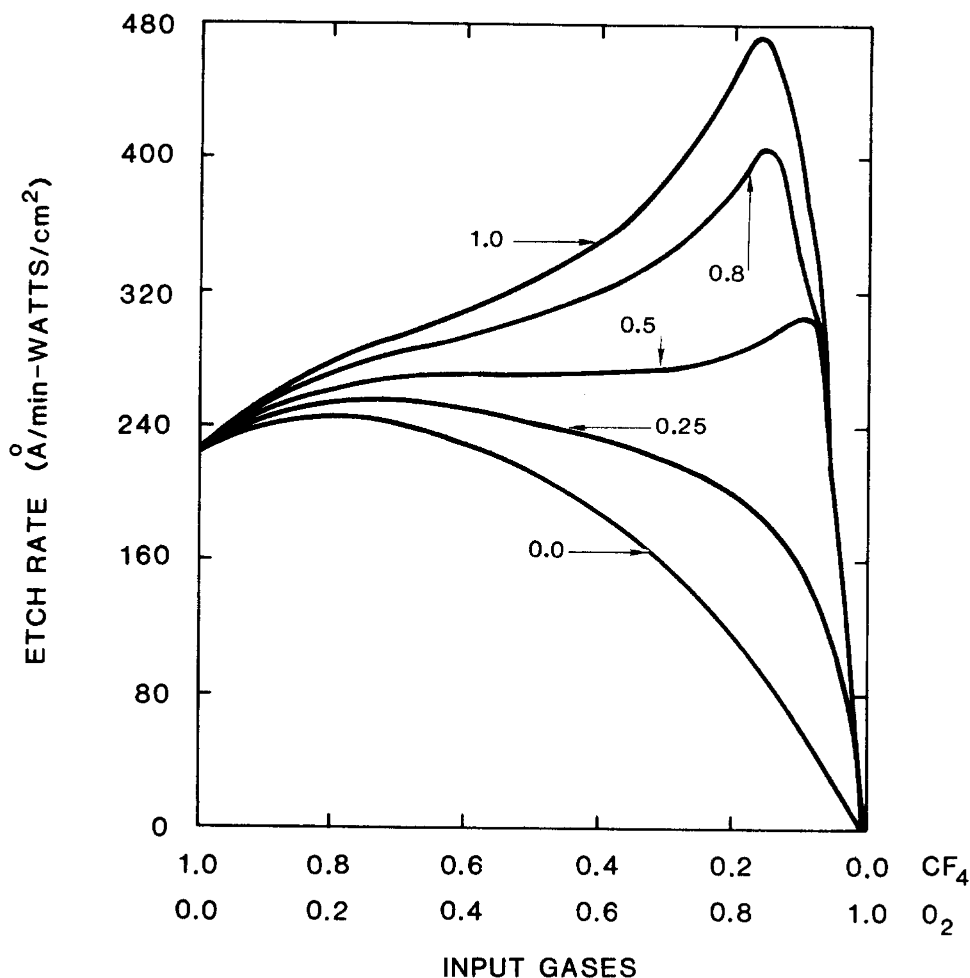

FIG. 15. Si etch rates computed as a function of the probability that adsorbed O and C are desorbed as CO. [This is the C-O analogy to reaction (22).] This process is an efficient cleansing mechanism and can greatly enhance the silicon etch rate.

for etching Si in C_nF_m/O_2 plasmas. These are reactions analogous to (23) which involve ions (e.g., dissociative charge exchange) and electron-impact dissociation of molecules such as COF and COF_2. The latter could be important, since the product of the dissociation is most probably atomic fluorine. The dissociation increases the adsorbable fluorine density without increasing the absorbable carbon density. Note that the importance of neutral reactions such as (4)–(8) increase as the ion and radical density decreases (i.e., low-powered plasmas). In these cases, the contribution of neutral gas-phase radicals to the etching process is large.

V. THE EFFECT OF ENHANCED ION FLUX ON SELECTIVITY

It has been discussed that despite the fact that ion densities are orders of magnitude smaller than the neutral radicals, their contribution to the etching process is 0.5–0.8 of the total. This is a result of their large mobilities and space-charge-enhanced ambipolar diffusion. It is clear that small changes in the ion density or local electic field can result in a large change in the ion flux, and hence a large change in the etch rate.

Comparing the C/F ratio of the ions to that of the neutral radicals, we find that the former is on the average twice that of the latter. The most abundant positive ions are CF_3^+ and CF_2^+, while F^+ has a small density due to its large ionization potential (17.4 eV). This results in a large C/F ratio for ions. The most abundant neutral radical is atomic fluorine, which results in a low C/F ratio. Therefore, if the positive ion flux to the vicinity of the substrate is increased, then the C/F ratio of the radical flux is increased and the etch rate of SiO_2 relative to Si is increased.

To investigate the affect of a change in the ion flux to a particular surface, a dc bias was imposed on the modeled plasma-etching reactor. This dc bias could be a self-bias[62] or an applied external field. The results of the calculation are shown in Fig. 16. As the applied dc electric field increases, the positive ion flux to the surface increases so that the C/F ratio of radicals arriving at the surface also increases. (Recall that the incremental ion flux is $\Delta E \cdot \Sigma_i \mu_i n_i$, where μ_i is the mobility ion i, n_i is the density of ion i, and ΔE is the change in electric field.) The result is that the selectivity of etching SiO_2 with respect to Si is increased. The limit to this process depends on the specific geometry and materials of the reactor. These factors determine the maximum dc field which can be generated or imposed on the discharge.

VI. CONCLUDING REMARKS

A kinetic model for the plasma-etching process has been presented which quantitatively describes the etching of silicon compounds in C_nF_m/H_2 and C_nF_m/O_2 plasmas. Good agreement with experiment has been obtained for the selective etching of Si and SiO_2 and for the abundances of neutral species in CF_4/H_2 plasmas. The preferential selectiv-

Downloaded 27 Mar 2003 to 128.174.115.149. Redistribution subject to AIP license or copyright, see http://ojps.aip.org/japo/japcr.jsp

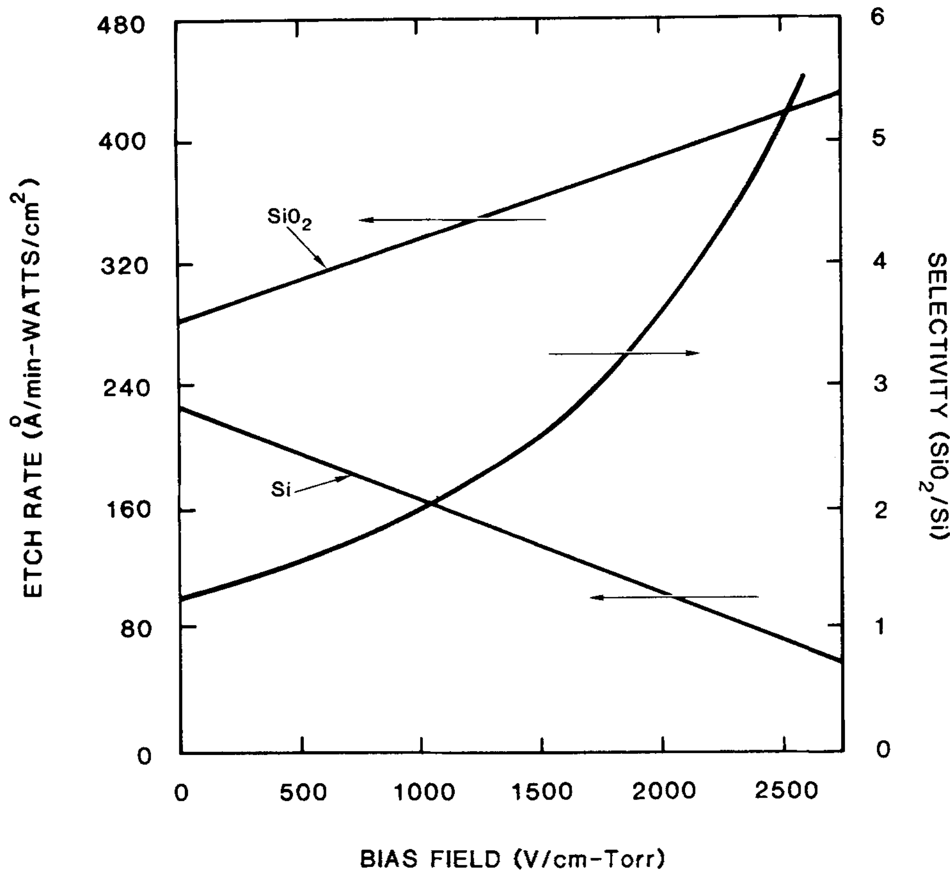

FIG. 16. By imposing a dc bias on the reactor, the C/F ratio of the radical flux arriving at the surface increases. This is due to the larger C/F ratio for ions with respect to neutral radicals. The change in the ratio increases the selectivity of etching SiO_2 with respect to Si.

ity of etching SiO_2 in C_nF_m/H_2 plasmas and Si in C_nF_m/O_2 plasmas has been found to be a sensitive function of the adsorption on the surface to be etched of atomic hydrogen and oxygen generated in the plasma. In the case of etching Si in CF_4/O_2 plasmas, this may be a dominant factor. Due to their large relative mobilities, charged radicals can be made to dominate the etching process. Since positive ions have a larger C/F ratio than neutral radicals, large ion fluxes will preferentially etch SiO_2 with respect to Si.

In the calculation of electron collision rates, the products of molecular dissociation were ignored. Despite this first-level approximation, the results are in good agreement with experiment. This is probably a consequence of the large E/P applied to the reactor and the high average electron energy which is obtained (5–10 eV). Under these conditions, collisions which have low-energy thresholds and are resonant in character (e.g., vibrational excitation) are less important in describing the energy balance. High-threshold, nonresonant events (e.g., ionization and dissociation) which do not differ greatly in their relative energy dependence from species to species are more important.[22] In addition, the large variety of dissociation products may, in effect, average the particular differences of those products in describing the energy balance and contribute to the success of the first-order approximation made.

Although good agreement was obtained with experimentally measured downstream abundances of neutral species, the correlation between mass spectroscopic measurements and conditions in the plasma must be carefully made. The rapid reassociation of radical species as they leave the plasma (due to a rapid decrease in the dissociative temperature) biases the results of the probe measurement towards the stable species.

ACKNOWLEDGMENT

This work was supported by the United States Department of Energy.

[1]J. Hayes and T. Pandhumsoporn, Solid State Technol. **11**, 71 (1980).
[2]B. Chapman, *Glow Discharge Processes: Sputtering and Plasma Etching* (Wiley, New York, 1980).
[3]R. G. Poulsen, J. Vac. Sci. Technol. **14**, 266 (1977).
[4]R. A. H. Heinecke, Solid-State Electron. **18**, 1146 (1975).
[5]D. Flamm, Solid State Technol. **22**, 109 (1979).
[6]J. W. Coburn and E. Kay, IBM J. Res. Dev. **23**, 33 (1979).
[7]J. W. Coburn and H. F. Winters, J. Vac. Sci. Technol. **16**, 391 (1979).
[8]R. A. H. Heinecke, Solid-State Electron. **18**, 1146 (1975).
[9]C. J. Mogab, A. C. Adams, and D. L. Flamm, J. Appl. Phys. **49**, 3796 (1978).
[10]E. A. Truesdale and G. Smolinsky, J. Appl. Phys. **50**, 6594 (1979).
[11]E. A. Truesdale, G. Smolinsky, and T. M. Mayer, *ibid.* **51**, 2909 (1980).
[12]B. A. Ruby, J. Vac. Sci. Technol. **15**, 205 (1978).
[13]M. J. Vasile, J. Appl. Phys. **51**, 2503 (1979).
[14]R. G. Frieser and J. Nogay, Appl. Spectrosc. **34**, 31 (1980); W. R. Harshbarger, R. A. Porter, T. A. Miller, and P. Norton, *ibid.* **31**, 201 (1977).
[15]Ya. Ya. Kuzyakov and V. M. Taterskii, Opt. Spektrosk. [Opt. Spectrosc. (USSR)] **5**, 699 (1958); F. X. Powell and D. R. Lide, Jr., J. Chem. Phys. **45**, 1067 (1966); Ya. P. Koretski, M. M. Dymchenko, B. M. Dymshits, A. P. Krasidinikova, and T. M. Putvinskaya, Trij. Gos. Inst. Prikl. Khim. **64**, 73 (1970).

Downloaded 27 Mar 2003 to 128.174.115.149. Redistribution subject to AIP license or copyright, see http://ojps.aip.org/japo/japcr.jsp

[16]D. L. Flamm, J. Appl. Phys. **51**, 5688 (1980).
[17]H. F. Winters, *ibid.* **49**, 5165 (1978).
[18]H. Norstrom, R. Olaison, S. Berg, and L. P. Anderson, Solid State Technol. **127**, 2680 (1980).
[19]J. A. Thornton, J. Vac. Sci. Technol. **15**, 188 (1978).
[20]E. Eser, R. E. Ogilvie, and K. A. Taylor, *ibid.* **15**, 199 (1978).
[21]H. F. Winters, J. W. Coburn, and E. Kay, J. Appl. Phys. **48**, 4973 (1977).
[22]M. J. Kushner, J. Appl. Phys. **53**, 2939 (1982).
[23]V. F. Babal'yanta, F. B. Vurzel, and L. S. Polack, Sov. Phys. Tech. Phys. **18**, 1197 (1974).
[24]W. L. Morgan, *JILA Information Center Report No. 19* (JILA, Boulder, Colorado, 1979).
[25]L. J. Kieffer, *A Compilation of Electron Collision Cross-Section Data for Modeling Gas Discharge Lasers*, JILA COM-74--11661, Boulder, Colorado (1973).
[26]M. S. Naidu and A. N. Prasad, J. Phys. D **5**, 983 (1972).
[27]P. W. Harland and J. L. Franklin, J. Chem. Phys. **61**, 1621 (1974).
[28]H. Chen, R. E. Center, D. W. Trainor, J. Appl. Phys. **48**, 2297 (1977).
[29]M. Gryzinski, Phys. Rev. **138**, A336 (1965).
[30]L. Vriens, Phys. Rev. **141**, 88 (1966).
[31]H. M. Rosenstock, K. Draxl, B. W. Steiner, and J. T. Herron, J. Phys. Chem. Ref. Data **6**, Suppl. 1 (1977).
[32]Y. Itikawa, J. Phys. Soc. Jpn.**36**, 1121 (1974).
[33]P. J. H. Woltz and A. H. Nielsen, J. Chem. Phys. **20**, 307(1952).
[34]J. Rud, C. M. Richards, and H. L. McMurray, *ibid.* **16**, 67 (1948).
[35]R. E. Olson, J. R. Peterson, J. Moseley, *ibid.* **53**, 3391 (1970); R. E. Olson, F. T. Smith, and E. Bauer, Appl. Opt. **10**, 1848 (1971).
[36]J. O. Hirschfelder, C. F. Curtis, and R. B. Bird, *Molecular Theory of Gases and Liquids* (Wiley, New York, 1954).
[37]S. W. Benson, *Thermochemical Kinetics*, 2nd ed. (Wiley, New York, 1976).
[38]H. S. Johnston and C. Parr, J. Am. Chem. Soc. **85**, 2544 (1963).
[39]D. R. Stull and H. Prophet, *JANAF Thermochemicals Tables*, 2nd ed., NSRDS-NBS 37 (National Bureau of Standards, Washington, D. C. 1971).
[40]A. P. Modica and S. J. Silkes, J. Chem. Phys. **48**, 3283 (1968).
[41]A. P. Modica, *ibid.* **44** 1585 (1966).
[42]N. Basco and F. G. M. Hathorn, Chem. Phys. Lett. **8**, 291 (1971).
[43]G. O. Pritchard and J. R. Dacey, Can. J. Chem. **38**, 182 (1960).
[44]F. W. Dalby, J. Chem. Phys. **41**, 2297 (1964).
[45]Pyrodynamics **4**, 371 (1966).
[46]A. C. Lloyd and J. Heicklen, J. Chem. Phys. **43**, 871 (1965).
[47]V. F. Kochubei and F. B. Moiri, Kinet. Catal. (USSR) **10**, 405 (1969).
[48]J. C. Amphlett and E. Whittle, Trans. Faraday Soc. **63**, 2695 (1967).
[49]G. B. Skinner, and G. H. Ringrose, J. Chem. Phys. **43**, 4129 (1965).
[50]N. Cohen, *A Review of Rate Coefficients for Reactions in the* H_2-F_2 *Laser System*, Aerospace Corporation TR-0073 (3430)-9, 1973.
[51]P. J. Hargis and M. J. Kushner *Detection of* CF_2 *Radicals in a Plasma Etching Reactor by* KrF *Laser-Induced Fluorescence Spectroscopy* (to be published).
[52]M. A. A. Clyne and R. T. Watson, J. Chem. Soc. Faraday Trans. 1 **70**, 1109 (1974).
[53]F. Westly, Table of *Recommended Rate Constants for Chemical Reactions Occurring in Combustion*, NBSIR 79-1941 (National Bureau of Standards, Washington, D.C., 1979).
[54]K. G. P. Sulzmann, B. F. Myers, and E. R. Bartle, J. Chem. Phys. **42**, 3969 (1965).
[55]S. C. Lin and W. I. Fyfe, Phys. Fluids **4**, 238 (1961).
[56]V. N. Kondratiev, *Rate Constants of Gas Phase Reactions*, COM-72-10014 (National Bureau of Standards, Washington, D.C., 1972).
[57]D. Saunders and J. Heicklen, J. Phys. Chem. **70**, 1950 (1966).
[58]M. A. A. Clyne and J. A. Coxon, Trans. Faraday Soc. **62**, 2175 (1966).
[59]G. L. Tingey, J. Phys. Chem. **70**, 1406 (1966).
[60]J. Verdeyan (private communication) 1981.
[61]J. N. Pitts, H. J. Sandoval, and R. Atkinson, Chem. Phys. Lett. **29**, 31 (1974). R. Atkinson, G. M. Breven, J. N. Pitts, and H. J. Sandoval, J. Geophys. Res. **81**, 5765 (1976).
[62]One electrode can be biased with respect to the other if their areas are different. This is called the area theorem. See Ref. 2 and J. W. Coburn and E. Kay, J. Appl. Phys. **43**, 4965 (1972).

Downloaded 27 Mar 2003 to 128.174.115.149. Redistribution subject to AIP license or copyright, see http://ojps.aip.org/japo/japcr.jsp